Available online at www.sciencedirect.com

ScienceDirect

Procedia Engineering 166 (2016) 229 – 246

Procedia Engineering

www.elsevier.com/locate/procedia

2nd International Symposium on Submerged Floating Tunnels and Underwater Tunnel Structures

Submerged Floating Tunnels under Seismic Motion: Vibration Mitigation and Seaquake effects

Luca Martinelli[a]*, Marco Domaneschi[a], Chunxia Shi[b]

[a]*Politecnico di Milano, Dep. of Civil and Environmental Engineering, Piazza Leonardo da Vinci 32, 20133 Milano, Italy*
[b]*Professional Engineer, Shanghai, PRC*

Abstract

In this work the activity of the research group active at Politecnico di Milano in the field of the dynamic behavior of Submerged Floating Tunnels (SFTs) is reviewed, with emphasis on the possibility to mitigate the dynamic response through structural control solutions and the modeling of seaquake effects.
A SFT model, equipped with suitable passive control devices, is accounted as a case study to assess the vibration mitigation under strong seismic motions. Elastic-plastic axial springs restrain the tunnel at the shores, and bars made of inelastic material anchor the tunnel to the seabed.
Earthquake and seaquake motions are introduced accounting for spatial variability of the seabed motion during an earthquake.
Some conclusions are drawn from a comparison between the response of the case study SFT due to earthquake and earthquake plus seaquake, which point out as seaquake forces can be an important source of excitation for SFTs. The paucity of studies on this topic, as well as the extent of the effects induced, call for further researches and developments.

Peer-review under responsibility of the organizing committee of SUFTUS-2016

Keywords: submerged floating tunnel; earthquake; seaquake; structural control

1. Introduction

Submerged Floating Tunnels (SFTs), also named Archimedes Bridges, are a promising alternative to cross body of water, efficiently connecting the shores while being entirely immersed. As such, they can have a very low impact

* Corresponding author. Tel.:+39-(0)2-2399-4247; fax: +39-(0)2-2399-4220.
E-mail address: luca.martinelli@polimi.it

Peer-review under responsibility of the organizing committee of SUFTUS-2016
doi:10.1016/j.proeng.2016.11.546

on the landscape. The first proposal about SFTs was formulated by S. Preault in 1860, later the concept caught the attention of several specialists from Italy, China, Norway, Japan, USA and other countries, becoming the object of a working group for SFTs established in 1989 [1] as well as of a specific sino-italian cooperation within the SIJLAB project.

Submerged Floating Tunnels (SFTs) are an intrinsically slender structural system that share some of the problems affecting other more traditional flexible systems for crossing bodies of water, such as suspended or cable-stayed bridges. The dynamic behavior shows some features which are typical of slender bridges as well, since in both systems the interaction between the main element (deck or tunnel) and the supporting elements (stays or anchoring elements) plays an important role and the performance under dynamic loads represents one of the most important factors affecting both feasibility and basic design choices. However, differently from bridges, earthquakes induce in SFTs not only inertia forces but also hydrodynamic fluid-structure interaction effects (seaquake). The term seaquake denotes here the hydrodynamic excitation related to the vertical transmission of compressive fluid waves activated by the seabed, which moves under seismic conditions.

Even though these systems can claim a good performance against seismic events, the complex loading conditions on SFTs can induce responses difficult to cope with in terns of safety or reliability. In this respect, structural control solutions can help to meet the required high standards of safety, mitigating the tunnels responses and protecting the main structural elements. Indeed, several fruitful applications of passive and semi-active control systems to long span structures, such as cable-stayed and suspension bridges under seismic loading (e.g. [2-5,12]), seem promising also when SFTs are considered. A more general review on design and modelling issues about SFTs can be found in the review work by Perotti et al. [6].

In seismic analysis, both the earthquake loads due to direct ground motion transmission to the structural supports and the so-called “seaquake” loading, due to the transmission through water of compressive waves originated at the seabed, are worth more attention. While the study on the dynamic response of SFTs subjected to strong seismic motion made significant progress in the last decades (e.g. Di Pilato et al. [7,8,], Martinelli et al. [9, 10], Shi et al. [11]), for seaquake research work on SFTs has only recently been started (see e.g. Shi [13] Shi & Martinelli [14], Shi et al. [15] or, more recently, [16]). Some studies on the effects of seaquake, however, were nevertheless available in the literature for a number of other different structural cases, which called for attention to the effects of propagating seismic waves in water due to seaquakes, and to the potential damaging effects that such waves could have (e.g. for offshore structures and floating systems, Hove et al. [17]). As a new type of external loading, this load works as a hydrodynamic pressure due to compression waves, since water cannot transmit shear waves, traveling through the water and excited by the motion of the seabed during an earthquake.

In this light, this paper reviews the activity of the research group active first at the Dep. of Structural Engineering (DIS) at Politecnico di Milano, and now at the Dep. of Civil and Environmental Engineering (DICA) of the same, with respect to modeling of seaquake effects and the possibility to mitigate the SFTs dynamic response through structural control solutions.

In the paper, the first part is devoted to introducing a SFT model, equipped with suitable passive control devices, which is accounted as a case study to assess the vibration mitigation issues under strong seismic motions. The numerical model is developed inside the commercial finite element (FE) framework ANSYS [18]. The elastic-plastic axial springs, which restrain the tunnel at the shores, and bars made of inelastic material, which anchor the tunnel to the seabed, act as passive control devices. The earthquake and seaquake motions accounts for the spatial variability of the seabed motion during an earthquake. This is an important aspect since SFTs lend themselves naturally to the crossing of large body of water, due to inherent modularization of the structure, and can reach dimensions in plan of the order of some kilometers. Finally, some conclusions are drawn from a comparison between the response of the case study SFT induced by “*earthquake*” and “*earthquake plus seaquake*”.

2. Assumed structural configuration and design criteria

Owing to the peculiar location, SFTs require that several research fields have to be covered to give a thorough view of their dynamic loading and of the resulting structural behavior, such as:

- seismic engineering analysis (for both support-transmitted and fluid-transmitted loads),

- fluid-structure interaction (for the definition of forces due to seaquake, sea waves and vortex shedding),
- vehicle-structure interaction (for the forces due to traffic loading),
- fast dynamics (for phenomena related to impact and explosions, both internal and external).

The numerical simulation of these phenomena involve delicate fluid-structure interaction aspects, and seems to be quite complex.

The studies presented in this paper and the related considerations refer to a design solution with the following characteristics:

- The tunnel axis is rectilinear and horizontal; the tunnel itself acts as a continuous beam.
- The anchoring system is provided by means of slender elements lying in a plane orthogonal to the tunnel axis; the anchoring elements are slender bars. Hollow cross section are selected so to lead to almost neutral conditions for the anchor elements under self weight and buoyancy effects, this resulting in an approximately straight configuration which positively affects the transverse initial stiffness of the SFT.
- In longitudinal (axial) direction the tunnel is restrained at both of the end sections. Special dissipation devices are assumed at these locations to avoid transmission of an excessive axial force in the tunnel.

As already pointed out in the cited review work by Perotti et al. [6], in such configuration, and for the type of loadings here considered, the tunnel dynamic response in the transverse and in the vertical plane is mainly affected by the behavior of the anchoring elements. In this light, an extensive analytical and numerical work has been performed by this research group aiming to the development of efficient and reliable models of these elements. Whenever the bending stiffness of the anchoring element is important two models have been developed: the first one (NWB element [19,20]) is capable of representing the entire anchor element, under the hypothesis of hinged end sections and constant axial force. The NWB element, though simplified, can capture the interaction between the transverse local oscillation of the bar, introduced through a variable number of local coordinates and shape functions, and the time varying axial force. The second model is a 3D beam finite element based on a corotational formulation [21]; upon discretization of the bar in a sufficient number of elements, the model allows for representing arbitrary large motions, though retaining the small deformation assumption. For the case of submerged tunnels anchored by cables [22,9], a previously developed finite element [23,24] has been adopted, especially in view of comparing the structural performance resulting from the two design strategies. This is a three-node cable element formulated in the large displacement and small deformation hypothesis. In the works reviewed in this paper, which are based on results from analyses carried out inside a commercial Finite Element environment, instead, the anchoring elements are modelled in a more classical way with four beam elements each.

The tunnel dead weight equals 1200 kN/m. The tunnel design criteria is bases on static buoyancy. The net buoyancy results in a pre-stressing state for the anchor bars, which are always in tension, under serviceability loads (the tunnel is designed so that the net static buoyancy is about 30%~40% of tunnel dead weight).

3. Model for hydrodynamic loads

In the numerical models here reviewed, the hydrodynamic loads on the SFT are due to current, and transmission of fluid waves due to earthquakes.

Notwithstanding the complexity of the fluid–structure interaction phenomena [8], in the works [11,14,15,25] here reviewed the Morison equation [26] is adopted to model the hydrodynamic forces (also that due to seaquake). This seems justified for the anchor bars given their diameter range while for the tunnel, the criterion seems justified when large waves are considered. In light of Morison approach, added mass effects are taken into consideration along with the structural mass working on the tunnel and anchoring system.

4. Control strategy

The traditional earthquake-resistant design is to ensure that the structure has enough strength, stiffness and ductility to resist the strong earthquake actions. However, other ways to protect structures against seismic external excitations can be also adopted, i.e. active and passive control.

Active control schemes require the installation of some specific devices aimed to collect monitoring data, to process them and to apply control forces.

Passive control allows for reducing the effects of earthquakes by decoupling the ground motion from the one of the structure and by dissipating part of the seismic energy through the hysteretic cycling behavior of special devices inserted into the structural system [27]. Passive control solutions have the benefit to simplify the implementation not requiring the monitoring and processing systems [28] and, as such, they appear suitable for adoption for SFTs.

In light of these considerations, the passive control system is implemented by including passive elastic-plastic devices connecting the tunnel to the shore. In most design proposals the tunnel itself acts as a continuous element, since no intermediate structural joints are allowed due to water tightness requirements. Consequently, dissipative devices can be applied only at the tunnel ends, trying to reduce the relative displacement between the structure and the shore though limiting the axial stress in the tunnel.

At the end sections, the tunnel is restrained against transverse and vertical motion, while flexural rotations are left free. The longitudinal displacements, relative to the abutment, iare controlled by the elastic-plastic springs defined in the following. The passive energy dissipation devices to be applied at the ends of the tunnel are modeled as nonlinear elastic-plastic springs. Their stiffness is derived from the yielding displacement and yielding force which are fixed respectively to 10cm and 5% of weight on the base of previous studies [29]. The post-yielding behavior is reasonably perfectly plastic.

With regard to the anchoring system, both elastic and inelastic materials are taken into consideration. These two options have been identified in the remaining of the paper as "*elastic*" and "*inelastic*". The steel elastic modulus is fixed to 2.06×10^5 MPa, the yielding stress to 2.10×10^8 N/m^2, and, when the inelastic behavior is implemented, the ratio between the post and the pre-yielding stiffness to 0.02.

5. Numerical models

In all the studies here reviewed [11,14,15,25] the following hypotheses and criteria have been adopted in developing a dynamic model of the complete structural system:

1. the tunnel is modeled as a single elastic beam; shear deformability is included; tunnel masses are lumped at anchoring sections;
2. soil-structure interaction effects are introduced by means of a lumped-parameter approach, encompassing frequency-independent spring and dashpots.
3. structural damping is introduced as Rayleigh damping.

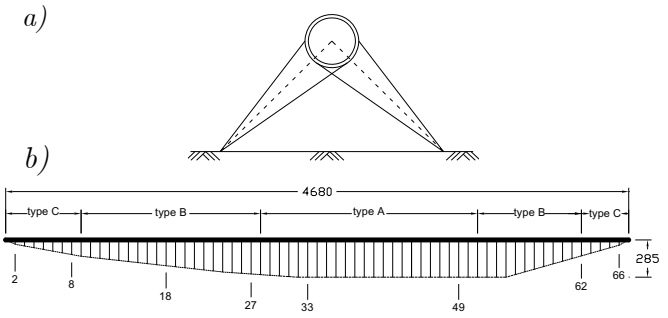

Fig. 1. (a) SFT schematic cross-section, (b) lateral view.

Table 1. Geometrical and Mechanical Characteristics of the Anchoring Bars.

Section	R_{out} (m)	R_{in} (m)	Area (m^2)	Second Area Mom. I (m^4)
A	0.933	0.871	0.348	0.139
B	0.975	0.910	0.385	0.171
C	1.029	0.963	0.425	0.211

Table 2. Geometrical and Mechanical Characteristics of Tunnel.

Outer diameter D_{out} (m)	Inner diameter D_{in} (m)	Area (m^2)	Second Area Mom. I(m^4)	Dead load (in dry conditions) of tunnel W (kN/m)
15.95	13.95	58.24	16370	1200

All of the analysis done to test the developed numerical models were relative to a design proposal (see Fig. 1) for a 4680 m Messina Strait Crossing between Punta S. Ranieri and Catona [30], with a maximum depth of about 325m and the tunnel set 40 m under the water level. The 3D finite element (FE) model of the SFT for the Messina Strait crossing was developed within the ANSYS software environment. The tunnel has a composite steel-concrete circular section and is connected to the seabed by means of slender steel beams having hollow circular section and pile foundations. In Tables 1 and 2, the geometrical and mechanical properties of the tunnel and of the anchor bars are listed.

In past works of the research group, employing ad-hoc developed elements, the anchoring system in was modeled using an equivalent bar on each side of the tunnel (broken line in Figure 1a). This bar had the same total cross-section area and second area moment of the two bars actually present on each side. In the works reported here [11,14,15,25] the SFT model was set up so that the anchoring system is simulated in a more realistic way with two bars for each side (solid lines in Figure 1a). Each bar is discretized with four beam elements from the ANSYS library [18].

The model accounts for soil-structure interaction, geometrical and material non-linearities as well as 3D multiple-support seismic excitation. The soil mechanical behavior is assumed as being linear.

Soil-structure interaction is modeled with elastic springs and dashpots, located at each end of the anchor bars (Fig. 2) and at the shore abutments. The stiffness coefficient K and damping coefficient C of these elements are listed in Table 3.

Table 3. Coefficient of the Soil-Structure Interaction for anchor bars and shore foundations.

Direction	Spring stiffness K (kN/m)	Damping coefficient C (kNs/m)
Horizontal	$2.87x10^6$	$2.66x10^4$
Vertical	$1.72x10^6$	$1.14x10^5$

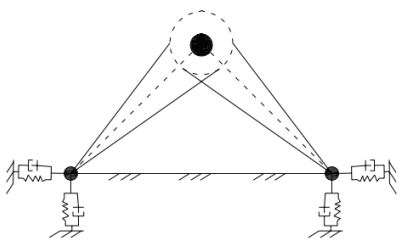

Fig. 2. Scheme for soil-structure interaction in transversal direction.

In transient analyses a Rayleigh damping has been selected for the models implemented inside the ANSYS environment. More refined damping models have been considered in [7-9]. These works, however, besides adopting specialized elements for the mooring structures made use of in-house developed computer codes that allowed more flexibility on the representation of damping forces.

ANSYS element COMBIN39 is used to simulate the nonlinear spring between the tunnel ends and the shores.

Fig. 3 depicts the first lateral mode shape of the SFT model, with the ends restrained as described.

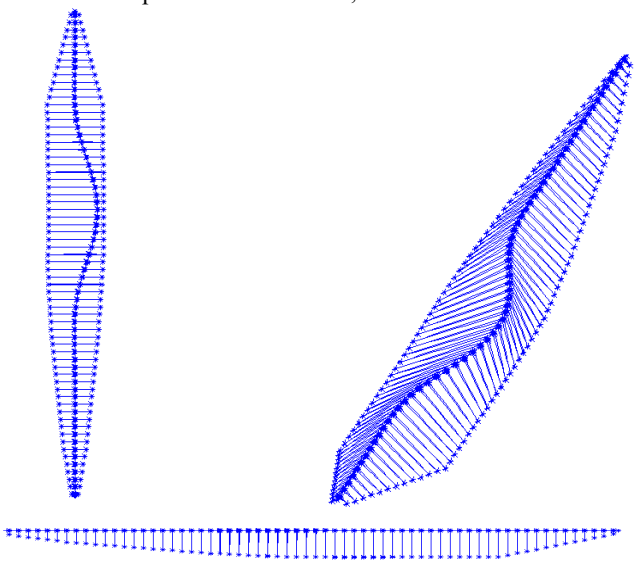

Fig. 3. First transversal mode-shape of the tunnel (0.580 Hz).

6. Seismic motion for the transient analyses

As the SFT has plan dimensions of the order of some kilometers, it must be considered to be subjected to partially correlated non synchronous seismic input motions at its supports. In the works here reviewed an artificial ground motion was considered. This is assumed as a realization of a space-time stochastic model based on a modified Kanai-Tajimi power spectral density.

6.1. Multi-support earthquake loading

The seismic excitation is applied at each ground connection points (shores and foundations of the anchoring bars) in the form of a multiple-support ground motion, first defined in terms of accelerations components. Artificial time histories of earthquake motion are generated in terms of transversal, vertical and longitudinal components at each support point, from these the displacements and velocities needed for the soil-structure interaction are derived by integration with suitable boundary conditions.

The seismic motion in terms of accelerations at a point is described by the Kanai-Tajimi power spectral density (PSD), as modified by Clough and Penzien [9,10].

The adopted PSD function for ground accelerations is expressed as in [9,10] as:

$$S(\omega) = S_0 S_{CP}(\omega)$$
$$= S_0 \frac{\omega_g^4 + 4\zeta_g^2\omega_g^2\omega^2}{(\omega_g^2 - \omega^2)^2 + 4\zeta_g^2\omega_g^2\omega^2} \frac{\omega^4}{(\omega_f^2 - \omega^2)^2 + 4\zeta_f^2\omega_f^2\omega^2} \quad (1)$$

where S_0 is the intensity of the ideal white noise process modelling the bedrock acceleration, $S_{CP}(\omega)$ the normalized Clough-Penzien spectrum, ω_g and ζ_g the characteristic ground frequency and damping, ω_f and ζ_f parameters of an additional filter introduced to guarantee finite power for displacements.
The parameters in Equation 1 have been selected according to the procedure presented in [9,10] and [34], to achieve acceleration time histories satisfying a code compatible response spectrum. The adopted values are ω_g 10 rad/s, ξ_g = 0.4, ω_f = 1.0 rad/s, ξ_f = 0.6.

A peak ground acceleration (PGA) of 0.64g has been adopted according to the study presented in [20] for the transversal and vertical directions, while 85% of this value was taken for the longitudinal direction.

The spatial variation of the ground motion is represented with the coherency model of Luco and Wong [32]. In this model the coherency function is defined in terms of the cross-power spectral density of ground acceleration between two stations i and j at a separation distance ξ_d :

$$\gamma(\xi_d, \omega) = \frac{S_{i,j}(\xi_d, \omega)}{\left[S_{i,i}(\omega) \cdot S_{j,j}(\omega)\right]^{1/2}} \quad (2)$$

where ω is the circular frequency, $S_{i,i}(\omega)$ and $S_{j,j}(\omega)$ the direct PSDs at the stations sites. The Luco and Wong model was adopted in the form:

$$\gamma(\xi_d, \omega) = \exp\left[-\left(\frac{\alpha_c \omega \xi_d}{v_s}\right)^2\right] \exp\left[i \frac{\omega \xi_d^{\,L}}{v_{app}}\right] \quad (3)$$

where ξ_d is the horizontal separation distance between stations i and j, v_s the velocity of the shear waves, α_c a parameter controlling the decay of the coherence, $\xi_d^{\,L}$ the projected horizontal distance between stations i and j along the wave propagation direction, v_{app} the apparent surface velocity of the "*dominant*" waves.

6.2. Seaquake loading

When seaquake effects are introduced, the hydrodynamic pressure is assumed associated with the seismic vibration transmitted through water from the seabed to the SFT. The velocity field due to the seaquake is derived form the velocity potential of the problem, which is deduced from the wave equation considering the free surface and seabed boundary conditions (Hamamoto [33], Takamura et al. [34], Shi [13]). The force on the moving body in the oscillatory flow is modeled by using Morison equation, which is adopted for simulating the seaquake loading on the tunnel [26].

The numerical simulation of the velocity field is carried out following the suggestions in [25].

7. Efficacy of the passive control strategy

By introducing inelastic material behavior in the anchoring bars, the effect of energy dissipation due to material hysteresis on the global response is estimated. Due attention is also devoted to the control of longitudinal oscillations of the tunnel, controlled by the end springs simulating the dissipative devices at the tunnel ends.

The results of the transient dynamic analyses are presented in the following subsections. The output from two structural configurations are compared, the one termed as "*Elastic*" assumes a linear elastic material behavior for the anchor bars while the one termed as "*Inelastic*" assumes an elastic-plastic behavior of the same. The seismic input consists of a single realization of seismic motion generated according to the criteria set forth in Section 6. The three components of the seismic motion are applied to the foundations of the anchor bars and at tunnel end abutments, without inclusion of the effect of seaquake.

7.1. Anchor Bars Response

Linear elastic and elastic-plastic behavior of the anchor bars is compared in Fig. 4. Fig. 4a shows the stress-strain curves obtained at the mid-span of one of the bar in the bracing plane closest to the shore, while Fig. 4b depicts the same curves for one of the bar in the bracing plane at the mid-span of the tunnel. Thicker solid lines represent results for the inelastic material behavior while the thinner dashed lines for the elastic one. The results in Fig. 4 have general validity, as it will be seen looking at the results of the analysis cases that include seaquake effects.

Even in this simplified analysis, that disregards seaquake effects, the bars closer to the shore show higher stress levels when the linear material behavior is implemented, or larger hysteretic cycles when the inelastic model is adopted. Compatibility with the local available ductility has to be checked. The bar located at the middle of the tunnel, instead, shows limited stress and ductility demand (Fig. 4b).

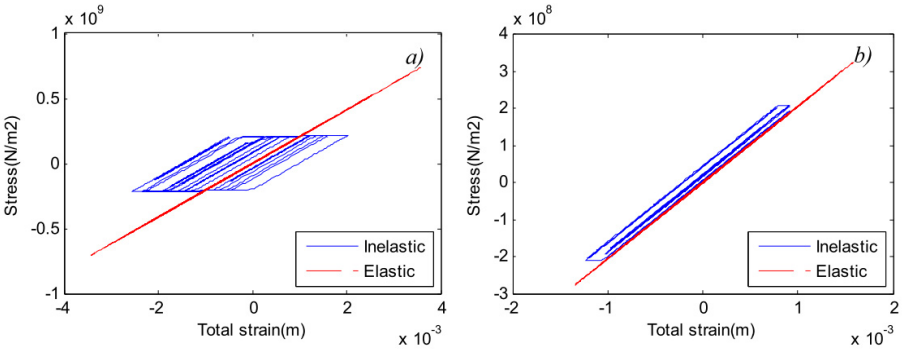

Fig. 4. Stress-strain relationship of the anchoring bars. (a) the bar nearest to the shore. (b) the bar at the middle of the tunnel.

7.2. Response of end springs

The nonlinear springs adopted as passive control devices at the tunnel ends, and that connect the tunnel and the shores, are implemented for dissipating part of the seismic energy and for decoupling the longitudinal ground motion of the SFT with the seismic one of the shores. Figure 5 depicts the device longitudinal displacement-force path at the tunnel end. Thicker solid lines represent results for the inelastic material behavior of the anchor bars while the thinner dashed lines for the elastic one.

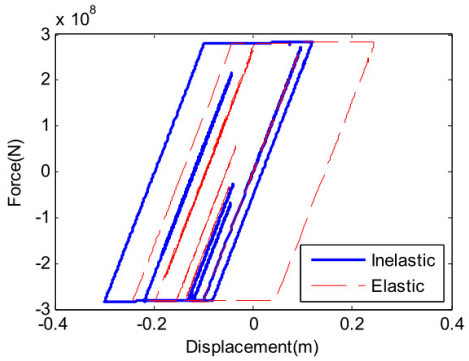

Fig. 5. Nonlinear behavior of the elastic-plastic spring at the shore.

7.3. Tunnel response

Results in terms of vertical (y), longitudinal (z) and transversal (x) absolute displacements, together with bending stress at the top-position in the tunnel section, are reported in Figs. 6-8 at three significant locations along the longitudinal tunnel axis: at the mid-span, at the quarter-span and near to the shore. Thicker solid lines represent results for the inelastic material behavior while the thinner dashed lines for the elastic one.

The vertical and transversal tunnel displacements are larger at the mid-span and at the quarter-span when compared to the shore. This outcome can be justified by considering the higher stiffness characterizing the anchor bars near to the shore, and gives also reason for the higher elastic stresses depicted by Fig. 4a with respect to the results in Fig. 4b.

The longitudinal tunnel displacements show little difference among the three locations considered. This is justified by the almost rigid body motion of the tunnel in the longitudinal direction accordingly to the kinematic constraints coming from the orientation of the anchor bars that will react in the longitudinal direction only due to second order effects, and hence to very large displacements. The overall displacements amplitudes are around 1m, still a small value with respect to the bars length over most of the length of the tunnel.

The material properties of the anchoring bars, finally, affect the tunnel response in terms of stresses. This is evident particularly at the mid-span and the quarter-span where the material inelastic behavior of the bars is able to reduce the bending stresses in the SFT cross-section. This is an interesting result given the mandatory water-tightness requirements adopted in the design.

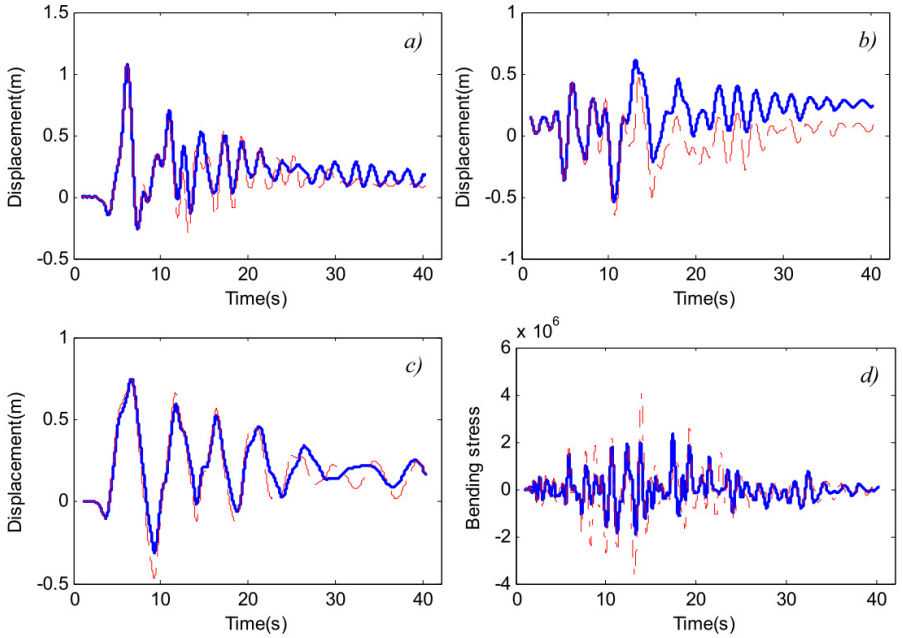

Fig. 6. Tunnel Mid-Span. Transversal Displacement (a), Vertical Displacement (b), Longitudinal Displacement (c), Bending Stress (d).

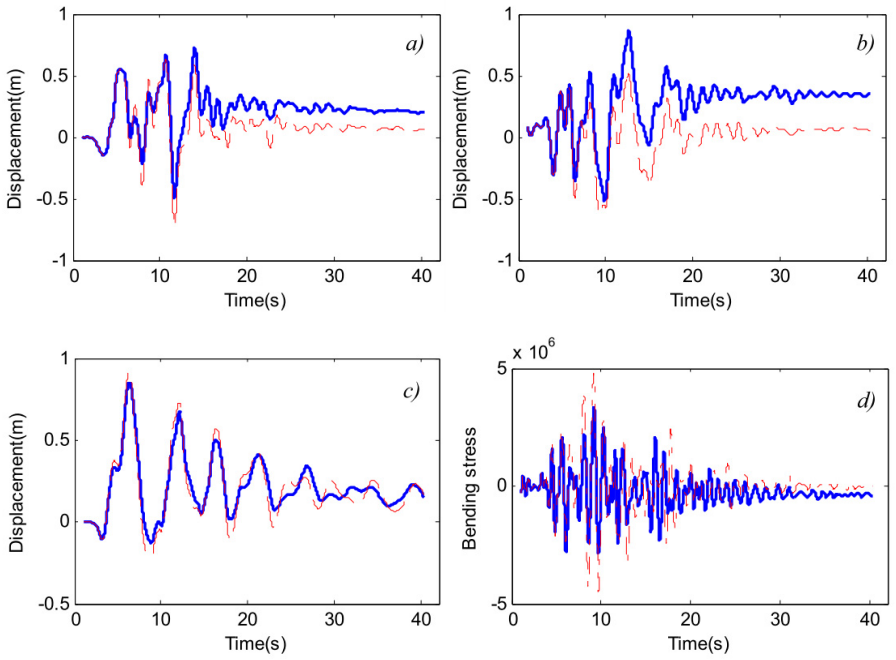

Fig. 7. Tunnel Quarter-Span. Transversal Displacement (a), Vertical Displacement (b), Longitudinal Displacement (c), Bending Stress (d).

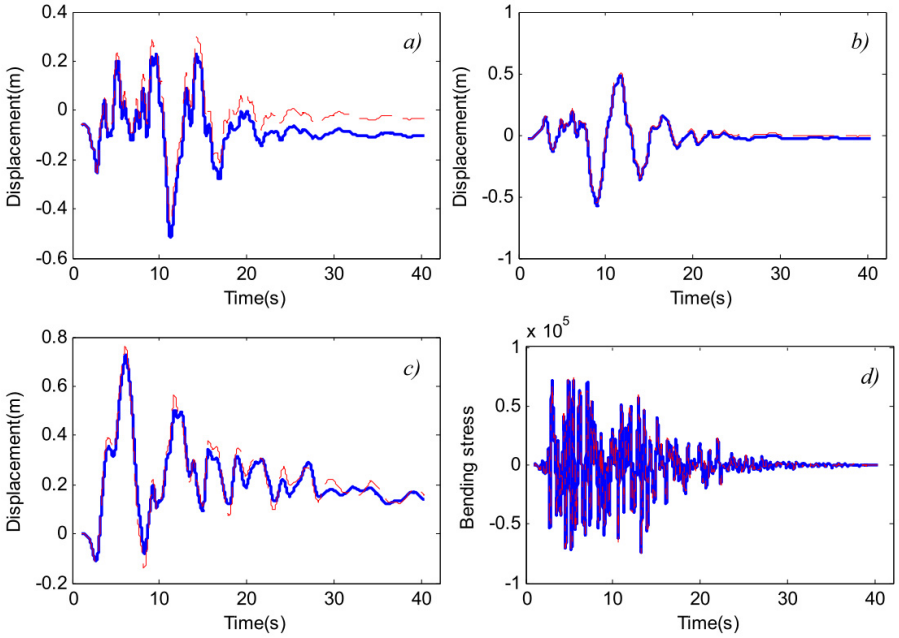

Fig. 8. Tunnel, near the Shore. Transversal Displacement (a), Vertical Displacement (b), Longitudinal Displacement (c), Bending Stress (d)

8. Effects of seaquake

Two different loading conditions have been implemented for the dynamic analyses: the first which accounts for the earthquake excitation is identified in the remaining of this section as the "*Eq*" one, the second is the superposition of both earthquake and seaquake excitations as is identified as the "*Sq+Eq*" one.

The transient dynamic responses of the passive control devices at the tunnel ends, the tunnel itself and the anchor bars under such loading conditions are presented in the following. The results shows how seaquake loading affects the responses of anchor bars, shore connections and tunnel sections in terms of stresses, forces and displacements. The results will show how a larger displacement capacity is required to the control system in the mitigation of dangerous structural responses, and the need of further investigations on seaquake effects.

In the following figures a solid line represents the responses under the combination of seaquake and earthquake excitations while a dashed line stands for the responses under earthquake only excitation. The behavior of the anchor bars is inelastic.

8.1. Anchor Bars Response

In Fig. 9, the inelastic behavior of the anchor bars is depicted. Fig. 9a shows the strain-stress relationship at the mid-section of the bar close to the shore; Fig. 9b gives the mid-section of the bar at the quarter-span of tunnel; meanwhile Fig. 9c the mid-section of the bar at the mid-span of tunnel.

From the general overview of these figures it arises that, while the seaquake effect severely influences the behavior of the anchoring system causing a significant strain increment in the bars at the middle span, in general larger hysteretic cycles are induced by the "*Sq+Eq*" loading also at other positions.

The bars close to the shore show ten times larger plastic deformations if compared with those at quarter-span and mid-span. This trend of higher plastic strains near the shores is general for both loading conditions and is related to the shorter length of these bars. The shorter bars display similar values of stress in compression and in tension, while the cycles for the longer bars is shifted on the tension side.

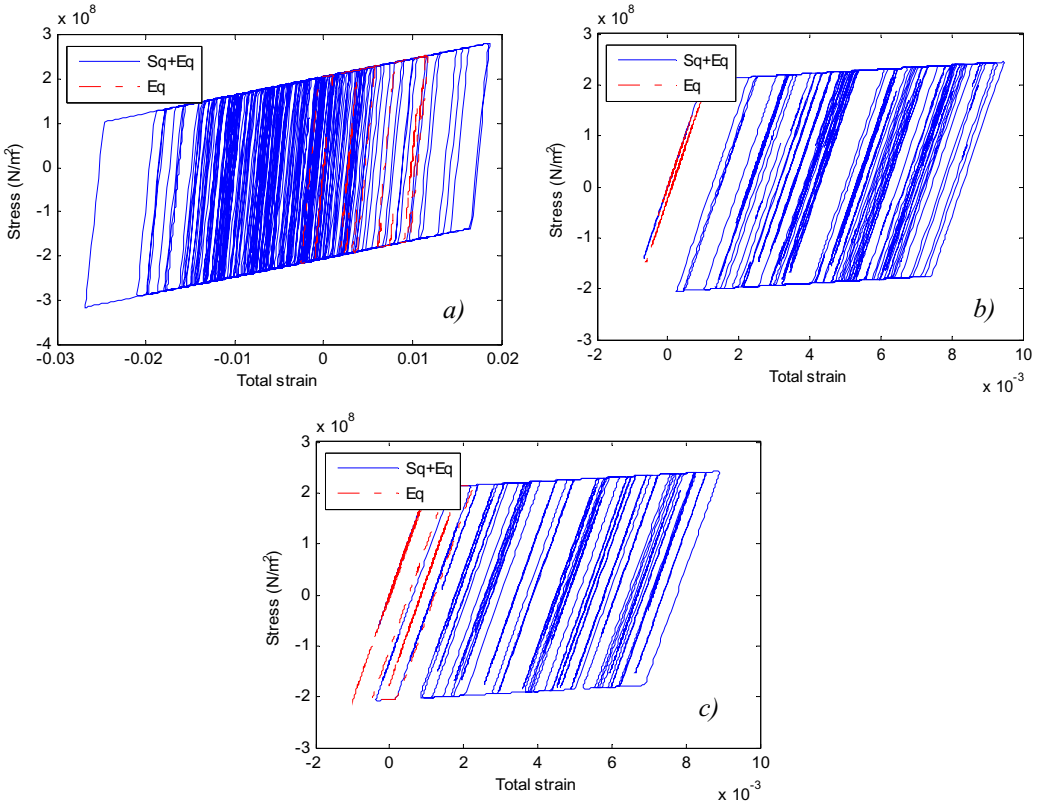

Fig. 9. Strain-stress relationships of anchoring bars: the mid-section of bar close to the shore (a), at the quarter-span of tunnel (b), at the mid-span of tunnel (c).

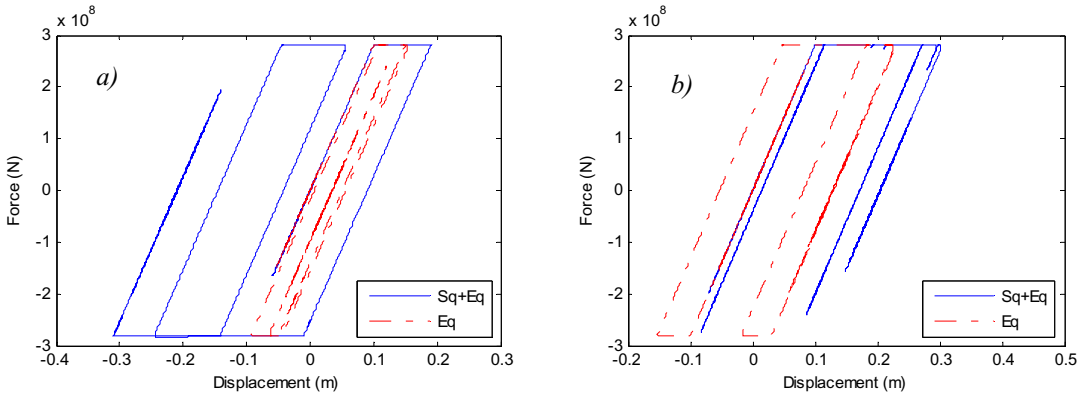

Fig. 10. Nonlinear behavior of elastic-plastic axial springs at tunnel ends.

8.2. End springs response

Fig. 10 reports the force-longitudinal displacement curves for the devices at both tunnel ends.

The passive control devices at the tunnel ends, both in cases of seaquake plus earthquake excitation ("*Sq+Eq*") and or earthquake only ("*Eq*"), dissipate satisfactorily the seismic energy through hysteretic cycles. Larger displacements can be detected for the "*Sq+Eq*" excitation case with respect to the simpler "*Eq*" case. This result highlights once more the more severe condition represented for the SFT by the coupled earthquake and seaquake excitation.

8.3. Tunnel response

Figs 11-15 depict the outcomes of the tunnel responses at the three locations along the longitudinal tunnel axis previously considered also for the anchoring bars (close to the shore, at the quarter-span, and at the mid-span). The response is given in terms of vertical (*y* axis), longitudinal (*z*) and transversal (*x*) absolute displacements, together with bending stresses (at top-position and side-position in the tunnel cross-section).

By looking at Fig. 11 one can appreciate as the transversal displacements of the tunnel sections show similar time variation for the "*Sq+Eq*" case as those in the "*Eq*" one at all the three positions considered. This means that the vertical loading due to the seaquake has a small influence in the transversal direction for the inelastic model here studied.

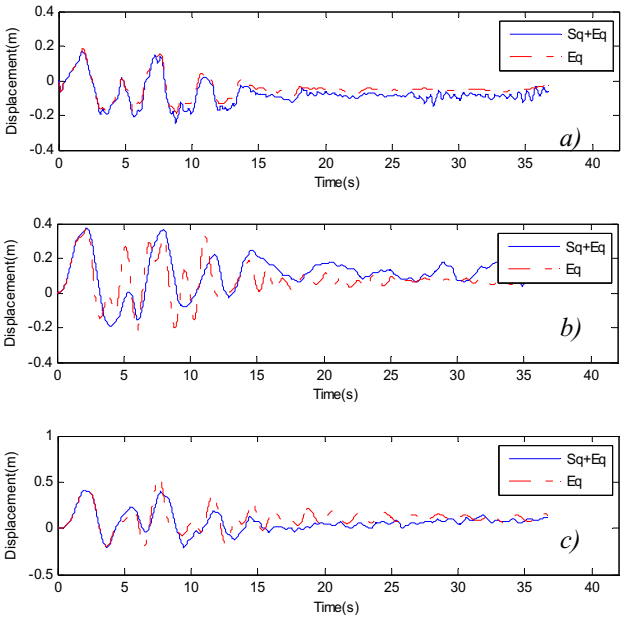

Fig. 11. Transversal displacement at tunnel section close to the shore (a), at the quarter-span (b), at the mid-span (c).

The vertical displacements are reported in Fig. 12. These show for the "*Sq+Eq*" loading case a drift in the tunnel sections at the quarter-span and at the mid-span and larger values than for the "*Eq*" case, particularly at the quarter and at the mid-span. The values are consistent with the strains in Fig. 9 and the bars length.

The longitudinal displacement depicted in Fig. 13 shows as well a drift in the tunnel sections near to the shore, at the quarter-span and at the mid-span. Particularly, the tunnel section near the shore shows the largest drift among the three sections, caused by the high yielding deformation in the anchoring bars near the shore and the proximity to the dissipative control devices.

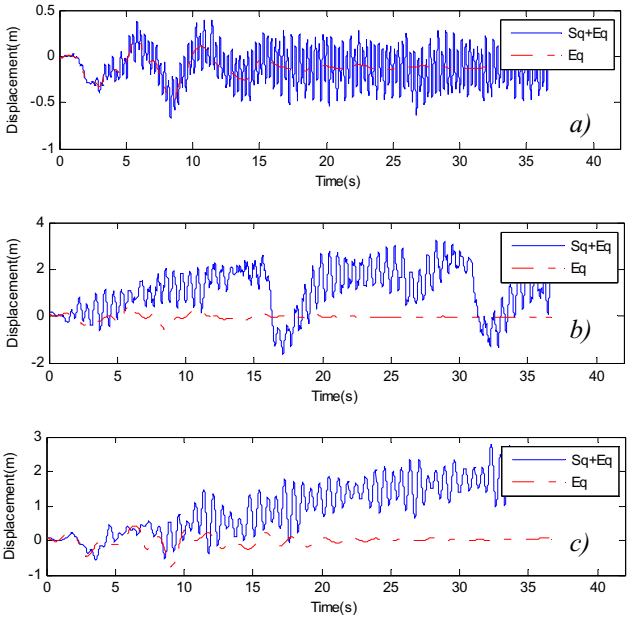

Fig. 12. Vertical displacement at tunnel section close to the shore (a), at the quarter-span (b), at the mid-span (c).

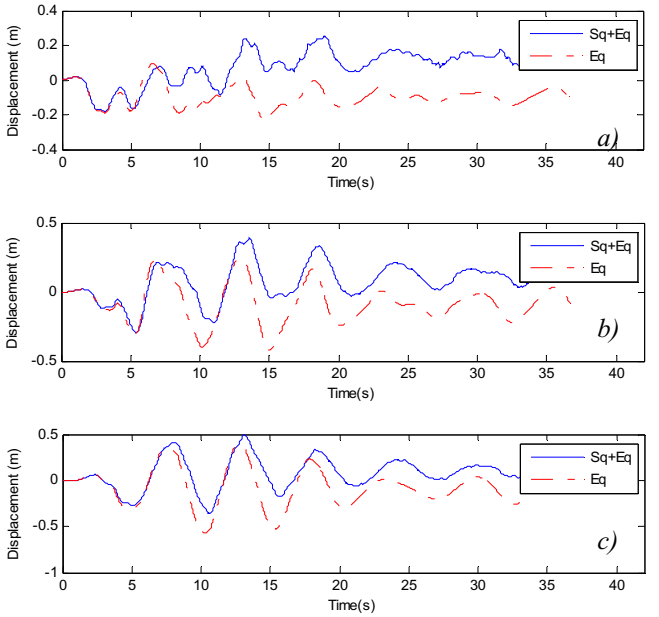

Fig. 13. Longitudinal displacement at tunnel section close to the shore (a), at the quarter-span (b), at the mid-span (c).

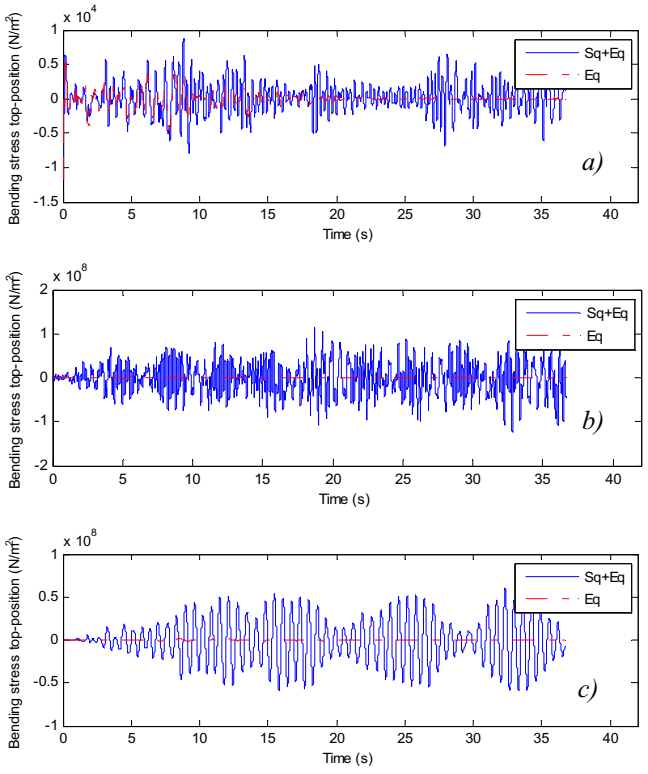

Fig. 14. Bending stress at top-position at tunnel section close to the shore (a), at the quarter-span (b), at the mid-span (c).

The larger effects of seaquake on the tunnel vertical motion are reflected also in the value of the stresses in the tunnel. Fig. 14 reports the bending stresses at the top of the tunnel cross-section at the three considered positions. The "*Sq+Eq*" loading case leads to larger values of the bending stress, enlarging to a large degree those due to earthquake only excitation.

Finally, by comparing the bending stresses in tunnel cross section side-position (depicted in Fig. 15) at the quarter-span and the mid-span, for the case "*Sq+Eq*" and "*Eq*", one can appreciate as the seaquake has little influence on the bending stress due to this position being close to the neutral axis for bending when the bending moment acts in the vertical plane.

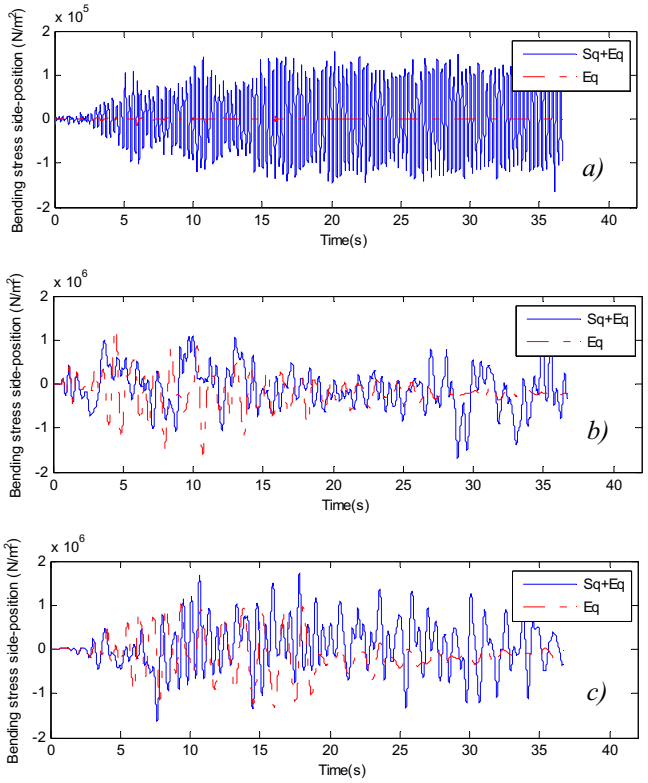

Fig. 15. Bending stress at side-position at tunnel section close to the shore (a), at the quarter-span (b), at the mid-span (c).

9. Conclusions

In the paper, results from literature works [11,14,15,25] of the research group on a 3D numerical model of a long SFT are reviewed. In these, a finite element model of a SFT has been studied under different earthquake excitations, namely the multi-support and the seaquake one, considering the spatial variability of the seabed motion during earthquakes.

The effect of controlling the SFT motion with dissipation devices are analyzed. Dissipation devices have been implemented (a) in the form of passive control devices at the tunnel ends, to control the axial force in the tunnel, and (b) by adopting inelastic materials laws for the bars that anchor the SFT to the seabed. In general, the dissipation devices implemented seems to perform efficiently, especially when both multi-support and seaquake loading are considered together.

Large axial forces have been detected in the anchor bars close to the tunnel ends, so that excursions in the nonlinear branch of their material behavior can appear as unavoidable. The anchoring bars largely exceed the yielding stress not only near the shore, where is can be expected due to the shorter length of the bars, but also at the quarter-span and mid-span along the tunnel.

The beneficial effects coming from the nonlinear behavior of the anchoring bars result in the reduction of the bending stresses in the tunnel sections, helping protecting this critical part form loss of water tightness requirements. The simulations points out, however, that even if of limited magnitude, the local ductility demands in the anchoring bars need nevertheless to be adequately checked.

The seaquake effect mainly induced a response in the vertical direction, affecting both vertical displacements and bending moments in the vertical plane. This is reflected in higher values of the bending stress at the cross-section top position.

Seaquake leads to and increased probability of damage both due to the higher stress in the tunnel and to the higher deformations in the mooring bars. This last consideration suggest (a) the need to pay to this source of excitation a larger attention in future designs and (b) the need of further researches to properly implement the "fuse-type" behavior required to the anchor bars to dissipate energy without imposing a too large inelastic deformation to these structural elements.

Acknowledgements

The authors are gratefully indebted to Prof. Federico Perotti, of Politecnico di Milano, for his inspiring talks and comments.

References

[1] C. Ingerslev, Immersed and floating tunnels. Procedia Engineering 4 (.2010) 51-59.

[2] M. Domaneschi, L. Martinelli, Performance Comparison of Passive Control Schemes for the Numerically Improved ASCE Cable-Stayed Bridge Model. Earthquakes and Structures 2 (2012) 181-201.

[3] M. Ismail, J. Rodellar, G. Carusone, M. Domaneschi, L. Martinelli, Characterization, modeling and assessment of Roll-N-Cage isolator using the cable-stayed bridge benchmark, Acta Mechanica 3 (2013) 525–547.

[4] M. Domaneschi, L. Martinelli, Refined optimal passive control of buffeting-induced wind loading of a suspension bridge, Wind and Structures, An International Journal, 1 (2014) 1-20.

[5] M. Domaneschi, L. Martinelli, F. Perotti, Wind and earthquake protection of cable-supported bridges, Proceedings of the Institution of Civil Engineers, Bridge Engineering BE3 (2016) 157–171, http://dx.doi.org/10.1680/bren.14.00026.

[6] F. Perotti, G. Barbella, M. Di Pilato, The dynamic behaviuor of Archimede's Bridges: numerical simulation and design implications, Procedia Engineering 4 (2010) 91–98.

[7] M. Di Pilato, A. Feriani, F. Perotti, Numerical models for the dynamic response of submerged floating tunnels under seismic loading, Earthquake Engineering and Structural Dynamics 9 (2008) 1203–1222.

[8] M. Di Pilato, F. Perotti, P. Fogazzi, 3D dynamic response of submerged floating tunnels under seismic and hydrodynamic excitation. Engineering Structures 30 (2008) 268-281.

[9] L. Martinelli, G. Barbella, A. Feriani, Modeling of Qiandao Lake submerged floating tunnel subject to multi-support seismic input, Procedia Engineering 4 (2010) 311–318.

[10] L. Martinelli, G. Barbella, A. Feriani, A numerical procedure for simulating the multi-support seismic response of submerged floating tunnels anchored by cables, Engineering Structures 33 (2011) 2850-2860.

[11] C. Shi, M. Domaneschi, F. Perotti, Submerged Floating Tunnels under seismic motion: vibration mitigation issues, in Proc. of 5th European Conference on Structural Control (EACS2012), Genoa, Italy, June 18-20, 2012.

[12] M. Domaneschi, L. Martinelli, C. Shi, Aeolic and seismic structural vibrations mitigation on long-span cable-supported bridges, Advanced Materials Research, 690 693 (2013) 1168-1171.

[13] C. Shi, Problems related to the seismic behaviour of Submerged Floating Tunnel, PhD Thesis in Structural, Earthquake and Geotechnical Engineering, XXV Cycle, Politecnico di Milano, 2013.

[14] C. Shi, M. Domaneschi, L. Martinelli, Nonlinear Behaviors of Submerged Floating Tunnels under Seismic Excitation, Applied Mechanics and Materials, 226-228 (2012) 1124-1127.

[15] C. Shi, M. Domaneschi, L. Martinelli, Nonlinear Behavior of Submerged Floating Tunnels Accounting for Seaquake Effects, in Proc. of the 5th International Conference on Structural Engineering, Mechanics and Computation (SEMC), CRC Press - Taylor & francis Group, 2013, 335-340.

[16] J. Mirzapour, M. Shahmardani, S. Tariverdilo, Seismic response of submerged floating tunnel under support excitation, Ships and Offshore Structures, (2016) DOI: 10.1080/17445302.2016.1171591.

[17] K. Hove, P.B. Selnes, H. Bungum, Seaquakes, A potential threat to offshore structures, in Proc. of the Third International Conference on Behaviour of Offshore Structures, Cambridge, USA, 1982, 561-571.

[18] Ansys Rel. 14 2012. Ansys Inc, USA.

[19] P. Fogazzi, F. Perotti, The dynamic response of seabed anchored floating tunnels under seismic excitation, Earthquake Engineering and Structural Dynamics, 3 (2000) 273-295.

[20] M. Di Pilato, F. Perotti, P. Fogazzi, 3D dynamic response of submerged floating tunnels under seismic and hydrodynamic excitation, Engineering Structures, 1 (2007) 268-281.

[21] M. Di Pilato, A. Feriani, F. Perotti, Numerical models for the dynamic response of submerged floating tunnels under seismic loading, Earthquake Engineering and Structural Dynamics, 9 (2008) 1203-1222.

[22] F.M. Mazzolani, R. Landolfo,.B. Faggiano, M. Esposto, F. Perotti, G. Barbella, Structural Analyses of the SFT Prototype on Qiandao Lake. Advances in Structural Engineering, 4 (2008) 439-454.

[23] L. Martinelli, F. Perotti, Numerical analysis of the non-linear dynamic behaviour of suspended cables under turbulent wind excitation, Int. Jour. of Structural Stability and Dynamics, 2 (2001) 207-234.

[24] V. Gattulli V, Martinelli L, Perotti F and Vestroni F. Nonlinear oscillations of cables under harmonic loading using analytical and finite element models, Comput. Methods Appl. Mech. Engrg., 1-2 (2004) 69-85.

[25] C. Shi, L. Martinelli, On the generation of seaquake velocity fields for submerged floating tunnel structures, Advanced Materials Research, 690 693 (2013) 1172-1175.

[26] S.K. Chakrabarti, Hydrodynamics of offshore structures, Computational Mechanical Publication, Southampton Boston, 1987.

[27] M. Dolce, D. Cardone, R. Marnetto, Implementation and testing of passive control devices based on shape memory alloys, Earthquake Engineering and Structural Dynamics, 7 (2009) 945-968.

[28] M. Domaneschi, L. Martinelli, Optimal passive and semi-active control of a wind excited suspension bridge, Structure and Infrastructure Engineering, 3 (2013) 242-259.

[29] C. Chilovi, Tunnel Flottanti In Alveo: Comportamento Dinamico e Soluzione Progettuali, MSc Thesis. Politecnico di Milano, Milano, Italy, 2008 (in Italian).

[30] R. Bruschi, V. Giardinieri, R. Marazza, T. Merletti, Submerged Buoyant anchored Tunnels: Technical Solution for the Fixed Link across the Strait of Messina Italy, in Proc. of Strait Crossings 1990. Balkema; Rotterdam.

[31] L. Martinelli, G. Barbella, A. Feriani, Multi-support seismic input gemeration: an harmonization with code prescriptions. In: Proc. of the 8th International Conference on Structural Dynamics, EURODYN 2011. Leuven, Belgio, 4-6 luglio 2011, ISBN/ISSN: 978907601931, European Association for Structural Dynamics (EASD), 2011.

[32] J.E. Luco, H.L. Wong, Response of a Rigid Foundation to a Spatially Random Ground Motion, Earthquake Engineering and Structural Dynamics, 6 (1986) 891-908.

[33] T. Hamamoto, Stochastic fluid-structure interaction of large circular floating islands during wind waves and seaquakes, Probabilistic engineering mechanics, 4 (1995) 209-224.

[34] H. Takamura, K. Masuda, H. Maeda, M. Bessho, A study on the estimation of the seaquake response of a floating structure considering the characteristics of seismic wave propagation in the ground and the water, J. of Marine Science and Technology, 4 (2003) 165-174.